Tracing the Electronic Pairing Glue in Unconventional Superconductors via Inelastic Scanning Tunneling Spectroscopy

Patrik Hlobil, Jasmin Jandke, Wulf Wulfhekel, and Jörg Schmalian

Tracing the electronic pairing glue in unconventional superconductors via Inelastic Scanning Tunneling Spectroscopy

Patrik Hlobil,[1,2] Jasmin Jandke,[3] Wulf Wulfhekel,[3] and Jörg Schmalian[1,2]

[1]Institut für Festkörperphysik, Karlsruher Institut für Technologie, 76344 Karlsruhe, Germany
[2]Institut für Theorie der Kondensierten Materie,
Karlsruher Institut für Technologie, 76131 Karlsruhe, Germany
[3]Physikalisches Institut, Karlsruher Institut für Technologie, 76131 Karlsruhe, Germany
(Dated: March 27, 2017)

Scanning tunneling microscopy (STM) has been shown to be a powerful experimental probe to detect electronic excitations and further allows to deduce fingerprints of bosonic collective modes in superconductors. Here, we demonstrate that the inclusion of inelastic tunnel events is crucial for the interpretation of tunneling spectra of unconventional superconductors and allows to directly probe electronic and bosonic excitations via STM. We apply the formalism to the iron based superconductor LiFeAs. With the inclusion of inelastic contributions, we find strong evidence for a non-conventional pairing mechanism, likely via magnetic excitations.

PACS numbers: 74.55.+v, 74.20.Mn, 74.20.Rp, 74.70.Xa

Electron tunneling spectroscopy has turned out to be an outstanding tool for the investigation of superconductors. A classical example is the determination of the electron-phonon pairing interaction in conventional superconductors [1, 2]. More recently, quasi-particles interference spectroscopy managed to exploit the local resolution of scanning tunneling microscopy (STM) to obtain momentum space information [3–5]. Both examples are based on elastic tunneling theory [6, 7] where one interprets the low-temperature conductance to be proportional to the electronic density of states (DOS), including renormalizations of the DOS that occur for example within the strong coupling Eliashberg formalism [8]. An energy dependent coupling to phonons or electronic collective modes and the details of these bosonic spectral features lead to a renormalization of the electronic DOS in form of peak-dip features above the superconducting coherence peaks [1]. Such pronounced peak-dip features have also been observed in cuprate and iron-based superconductors [9–13, 15–25]. A frequent interpretation is, based on elastic tunneling theory, in terms of a coupling of electrons to a sharp spin resonance mode with frequency ω_{res} and with momentum at the antiferromagnetic ordering vector of the material [26–28].

In an interacting system the injection of a real electron may cause both, the creation of a fermionic quasiparticle and the excitation of (bosonic) collective modes as depicted in Fig. 1. The strength of the interaction is usually crucial for the relative weight of the low-energy quasiparticle and the cloud of excitations associated with it. The excitation of the quasiparticle corresponds to the above discussed elastic tunneling, while the creation of real collective modes during the tunneling process corresponds to *inelastic tunneling*.

In this paper we demonstrate that such inelastic tunneling events can lead to important and observable modifications of the STM spectrum in unconventional su-
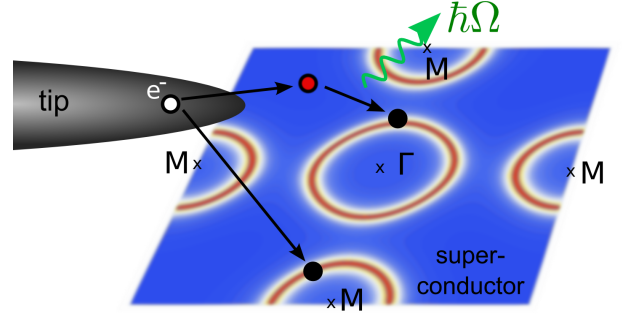

FIG. 1: Sketch of the elastic and inelastic tunneling processes from the tip (gray) to the band structure of the superconductor. An inelastic tunneling process involves an intermediate off-shell state far away from the Fermi surface (marked in red), from which the electron is scattered inelastically via the emission/absorption of a boson with frequency Ω to a state near the Fermi surface (black).

perconductors. In addition to fermionic exitations that are visible via elastic tunneling, inelastic tunneling spectroscopy can be used to identify the bosonic excitations of the system. We show that the fine-structures seen in LiFeAs are predominantly due to such inelastic tunneling processes and thus evidence of an electronic pairing source. Here, we analyze electronic pairing where the excitations causing superconductivity are directly related to the collective bosonic modes of the electrons themselves (e.g. electron-spin fluctuations). In the superconducting state, electrons open a gap Δ in their spectrum. This impacts all collective excitations of the electrons. In other words, collective spin and charge degrees of freedom inherit a gap in the bosonic spectrum below T_c. This behavior is shown in the Fig. 2, where numerical results for the calculated electronic and spin spectral function above and below T_c are shown [40–42]. The spin spectrum inherits a gap ω_{res} related to a resonance mode at this

energy. If the bosonic glue is made up of such a gapped spectrum, it will strongly affect the inelastic tunneling spectrum (much stronger than the elastic one).

An inelastic tunneling event is depicted in Fig. 1. A tip-electron tunnels elastically into a high-energy off-shell state far away from the Fermi surface from where the electron scatters inelastically via the emission/absorption of a boson to a state near the Fermi-surface. Inelastic tunneling has been observed for conventional superconductors in the normal state [30, 31] where it was shown, that tunneling electrons excite bulk phonons since the measured second derivative of the tunneling turned out to be proportional to the Eliashberg function ($d^2I/dU^2 \propto \alpha^2 F(\omega)$) which is given by the electron-phonon coupling constant α times the phonon spectrum $F(\omega)$. This inelastic contribution has recently been shown to be of importance even in the superconducting state of Pb-films (almost to the same extent) [33]. Furthermore, in the normal state of the cuprate superconductors it is well established that inelastic tunneling channels are present and in general not negligible [10, 21, 35–37, 39, 40]. They give rise to the frequently observed V-shape of the normal state spectrum closely tied to an overdamped particle-

hole spectrum as depicted by the blue curve in Figure 2. Such V-shaped background conductances have also been seen in the iron pnictide superconductors [13, 24, 25]. In the superconducting state inelastic tunneling was discussed in the context of fine structures of the tunneling spectrum that displayed an isotope effect, suggesting the tunneling via apical oxygen states [38]. We will show that inelastic tunneling below T_c can be utilized to narrow down the pairing mechanism in unconventional superconductors, where one expects a dramatic reorganization of the pairing glue spectrum in the superconducting state in contrast to the electron-phonon coupling case.

If one expands with regards to the usual tunneling matrix element $t_{\mathbf{k},\mathbf{p}}$ between tip and superconductor[55], the tunneling current $I = I^{\mathrm{e}} + I^{\mathrm{i}}$ consists of an elastic and inelastic contribution I^{e} and I^{i}, respectively. Both are of same order in tunneling $\mathcal{O}\left(t^2\right)$, yet the inelastic contribution may be suppressed in case of momentum conservation at the tunneling junction. Following our previous analysis for conventional superconductors [33] we find for $t_{\mathbf{k},\mathbf{p}} \approx t$, appropriate for STM geometries [29], and for a constant tip DOS the two contributions to the differential conductance $\sigma(U) = dI/dU$ [35, 36]

$$\sigma^{\mathrm{e}}(U) = -\sigma_0 \int_{-\infty}^{\infty} d\omega\, n_F'(\omega + eU)\tilde{\nu}_S(\omega)\,, \tag{1}$$

$$\sigma^{\mathrm{i}}(U) = -\frac{\sigma_0}{D^2\nu_S^0} \int_{-\infty}^{\infty} d\omega_1 d\omega_2\, g^2 \chi''(\omega_1)\tilde{\nu}_S(\omega_2) \Big[n_F'(\omega_2 - \omega_1 + eU)n_B(\omega_1)\big[1 - n_F(\omega_2)\big] + n_F(\omega_2)\big[1 + n_B(\omega_1)\big]n_F'(\omega_2 - \omega_1 + eU)$$

$$+ n_F'(\omega_2 + \omega_1 + eU)\big[1 + n_B(\omega_1)\big]\big[1 - n_F(\omega_2)\big] + n_F(\omega_2)n_B(\omega_1)n_F'(\omega_2 + \omega_1 + eU)\Big], \tag{2}$$

where U is the applied voltage, $\sigma_0 = 4\pi e^2 |t|^2 \nu_T^0 \nu_S^0$, g the coupling strength between the electrons and the collective mode and $\nu_{S/T}^0$ are the normal state DOS of the superconductor and the tip at the Fermi energy, respectively. D is some characteristic upper cut off for the bosonic excitation spectrum characterized by the imaginary part of the the momentum averaged propagator $\chi''(\omega)$. For a detailed derivation of these expressions see the supplementary information [32], where we demonstrate that the distinction between elastic and inelastic tunneling is due to the fact that the electronic spectrum is subdivided into a low-energy renormalized quasiparticle regime and high-energy off-shell states. Usually, many-body interactions are analysed for the renormalized quasiparticle excitations. However, tunneling processes into off-shell states far away from the Fermi surface may subsequently relax into states near the Fermi energy via the emission of a bosonic excitation. This is a process with a large phase space as long as the typical bosonic momentum is large. Examples are zone-boundary phonons or antiferromagnetic fluctuations.

We also point out that the relative phase space for

elastic and inelastic processes depends sensitively on the detailed tunneling geometry, i.e. whether one considers planar or point-contact junctions or an STM geometry. STM settings with poor momentum conservation [29] give large inelastic contributions.

In the following, we investigate, for a specific model, how inelastic tunneling affects the tunneling spectra in unconventional superconductors. We consider the case of a spin-fermion coupling proposed as an effective model for various unconventional superconductors [40]. The relevant collective bosonic degrees of freedom can be written in terms of a 3-component spin vector $\mathbf{S_q}$ with a Yukawa-like electron-boson coupling

$$H_{\mathrm{int}} = g \int dx\, c_\alpha^\dagger \boldsymbol{\sigma}_{\alpha\beta} c_\beta \cdot \mathbf{S} \tag{3}$$

with the Pauli-matrices σ^i. We also define the normalized electronic DOS $\tilde{\nu}_S(\omega) = \nu_S(\omega)/\nu_S^0$, the coupling constant g and the dimensionless, integrated spin spectrum $\chi''(\omega) = -3\nu_S^0 \int d^dq \mathrm{Im}\chi_{\mathbf{q}}(\omega)/\pi$. We solve this model self-consistently using the formalism of Ref. [40–42] which determines the superconducting gap-function
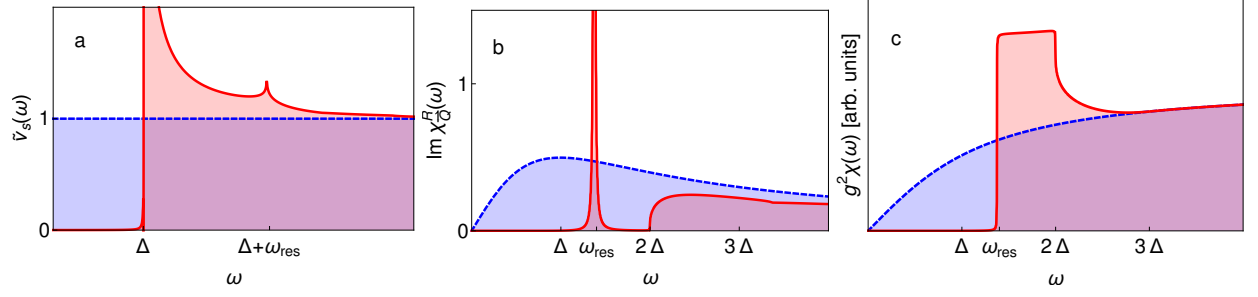
FIG. 2: **Calculated spectra for the spin electron model in the normal (blue) and superconducting state (red): a**, Electronic density of states. **b**, Spin spectrum $\mathrm{Im}\,\chi_Q^R(\omega)$ at the antiferromagnetic ordering vector Q with the resonance mode occurring at ω_{res} below T_c. **c**, spin spectrum $g^2\chi$ integrated over the 2-dimensional Brillouin zone.

and the renormalized electron and spin-fluctuation propagators. This Eliashberg treatment is well established and the coupled set of equations is given in Ref. [42]. The solutions are displayed in Fig. 2. Recent quantum Monte Carlo calculations confirmed that this approach is quantitatively correct as long as the dimensionless coupling constant is not much larger than unity [43].

We first analyze the normal state behavior. At sufficiently low T and for a structure-less density of states, Eq.(2) simplifies to

$$\sigma^{\mathrm{i}}(U) \propto g^2 \int_0^{eU} d\omega \chi''(\omega). \tag{4}$$

Above T_c the spin susceptibility shows an overdamped behaviour $\chi_{\mathbf{q}}(\omega)^{-1} \sim \xi^{-2} + (\mathbf{q} - \mathbf{Q})^2 - \Pi_{\mathbf{Q}}(\omega)$ with $\Pi_{\mathbf{Q}}(\omega) = i\gamma\omega$, where $\gamma \sim g^2/v_S^0$. Here, $\mathbf{Q}$ is the antiferromagnetic ordering vector and $\omega_{\mathrm{sf}} = \gamma^{-1}\xi^{-2}$ the characteristic energy scale of the boson. For $d = 2$ it follows $\chi''(\omega) = \frac{3}{2\pi}\nu_S^0 \arctan\left(\frac{\omega}{\omega_{\mathrm{sf}}}\right)$, which leads to $\sigma^{\mathrm{i}}(U) \propto g^2 U^2/\omega_{\mathrm{sf}}$ for small voltages ($eU \ll \omega_{\mathrm{sf}}$) and a linear dependence $\sigma^{\mathrm{i}}(U) \propto g^2\pi|U|$ for $eU \gg \omega_{\mathrm{sf}}$, yielding a natural explanation for the V-shaped (at low voltages rather U-shaped) spectrum [35, 36]. For $T > 0$, inelastic tunneling is also present at finite voltage and therefore increasing the purely elastic conductance to be larger than σ_0 at zero bias in Fig. 3 (c). Note, the same can be achieved within the bosonic spectrum that underlies the marginal Fermi liquid approach, where the role of ω_{sf} is played by temperature. As inelastic tunneling only probes the momentum-averaged bosonic spectrum it cannot discriminate between these two scenarios. Within the antiferromagnetic fluctuation theory it is however important that the effective dimensionality of the spin-excitation spectrum is $d = 2$. For arbitrary dimension follows in the regime $eU \gg \omega_{\mathrm{sf}}$ that $\sigma^{\mathrm{i}}(U) \propto |U|^{d/2}$, a behavior that occurs down to smallest voltages at an antiferromagnetic quantum critical point, where $\omega_{\mathrm{sf}} \to 0$, and may serve to identify the effective dimension of the spin-fluctuation spectrum in a given system. In Fig. 3 (a) and 3(b) we show in blue the elastic and inelastic con-

ductance obtained from the solution of the spin-fermion model above T_c. While the elastic contribution is constant for the normal state, the inelastic conductance of Fig. 3b) shows the expected V-shape structure. As discussed earlier [37, 39], inelastic processes open up additional tunneling channels for both positive and negative bias U. Most important for our considerations is that the observation of an V-shaped inelastic contribution in the normal state implies that it cannot be ignored in the superconducting state and allows for an estimate of its relative contribution.

We now turn to the superconducting state. We solve the Eliashberg equations for spin-fluctuation induced pairing numerically [44], considering a nodeless pairing state (see Fig. 2). This is appropriate for several iron based superconductors with $s^{\pm}$-pairing. For systems with nodes it mostly implies that we should confine ourselves to frequencies above the superconducting gap, which is the regime we are interested in anyway. As usual, the sign of the gap changes between states that are connected by the magnetic wave vector and the resonance mode at ω_{res} naturally occurs within our formalism. We have chosen our input parameters ω_{sf} and g of the theory in such a way that the observed gap and spin spectrum agrees well with the experimental observations [45–48] $\omega_{\mathrm{sf}} \simeq \Delta$ and $\omega_{\mathrm{res}} \approx 1.4\Delta$, where ω_{res} is the resonance mode seen by inelastic neutron scattering [46, 48–50] that has left traces in other experimental techniques as well [51–53]. We stress that the key conclusions of our analysis are not affected by changing the above parameters within reasonable ranges.

In the superconducting state, the following features arise in the tunneling spectrum: The *elastic* tunneling contribution seen in Fig. 3(a) (red curve) is proportional to the thermally smeared electronic DOS with the gap Δ, the coherence peak at Δ followed by the usual peak-dip strong-coupling features seen at $\Delta + \omega_{\mathrm{res}}$ that quickly approaches the assumed constant DOS of the normal state for higher biases. The *inelastic* tunneling conductance seen in Fig. 3b) (red curve) is gapped by $\Delta + \omega_{\mathrm{res}}$ as both the electronic DOS and the bosonic spectrum
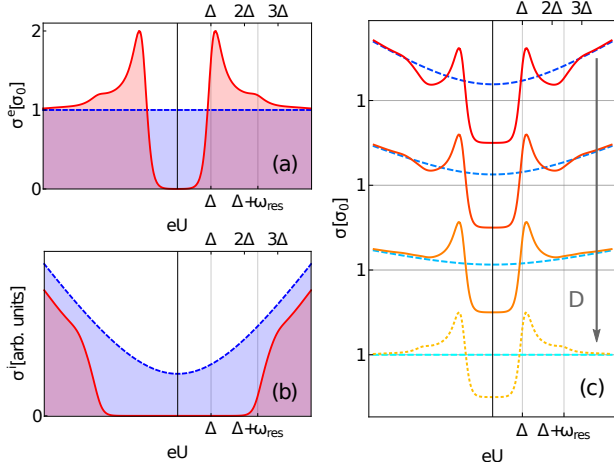
FIG. 3: Calculated elastic (a) and inelastic (b) contributions to the conductance both in the superconducting (red) and normal state (blue). In (c) the total tunneling spectra for different inelastic tunneling amplitudes are shown. We use $1/(D^2\nu_0^S) = (0, 0.2, 0.5, 0.8)\,1/\mathrm{meV}$ which are reasonbel values for systems with electronic pairing. The tunneling parameters are set such that the current I at $eU = 10\Delta$ is the same for the normal and superconducting state. The combination of elastic and inelastic contributions leads to the apperance of a dip feature, reflecting primarily the reorganization of the bosonic spectral weight below T_c of the inelastic tunneling contribution.

FIG. 4: Normalized conductance $\sigma_{\mathrm{norm}}(U) = \sigma_{\mathrm{sc}}(U)/\sigma_{\mathrm{nc}}(\sqrt{U^2-(\Delta/e)^2})$ (upper panel) and derivative of the normalized conductance (lower panel). We use the same values for $1/(D^2\nu_0^S)$ as in Fig. 3 (c). Left we show our theoretical results, compared to the STM data of LiFeAs from Ref. [13] on the right. In the upper right panel, colors indicate a temperature evolution from $2\,\mathrm{K}$ (black) to $16.5\,\mathrm{K}$ (red). The observed fine structures near $\Delta + \omega_{\mathrm{res}}$ require a significant contribution of inelastic tunneling events. These structures require an electronic pairing mechanism with pairing glue gapped below T_c. The signatures of the resonance mode require a sign changing pairing state.

obtain a gap below T_c. For voltages $eU > \Delta + \omega_{\mathrm{res}}$ the inelastic differential conductance shows a sharp increase. This behavior can be traced back to the fact that spin spectral weight is shifted from lower to higher energies, mostly close above the resonance mode at the frequency ω_{res}. For our calculations we have chosen our temperature $T = 0.1\Delta$ in the superconducting state and $T = 0.5\Delta$ in the normal state, where Δ is the gap at zero temperature.

Naturally, only the sum $\sigma = \sigma^{\mathrm{e}} + \sigma^{\mathrm{i}}$ is observable in tunneling experiments. Fig. 3(c) depicts the resulting total conductance including the normalization for different energy cutoffs D. We set the tunneling parameters such that the current I at $U = 10\Delta$ is the same for the normal and superconducting state. For weak inelastic contributions (g/D small) mainly the quasiparticle peak at Δ is visible on top of a small inelastic increase at high energies. Note, that the conductance in the superconducting state is always higher than in the normal state outside the gap. The Eliashberg-features of the resonance mode are already obscured by the inelastic contributions (second curve from below). If we increase the inelastic tunneling amplitude we see that the conductance in the superconducting state is lowered below the normal state at $eU \approx 2\Delta$ due to the loss of spin spectral weight. Note that in the normal state, both elastic and inelastic contributions are present while in the superconducting state, there are only elastic contributions
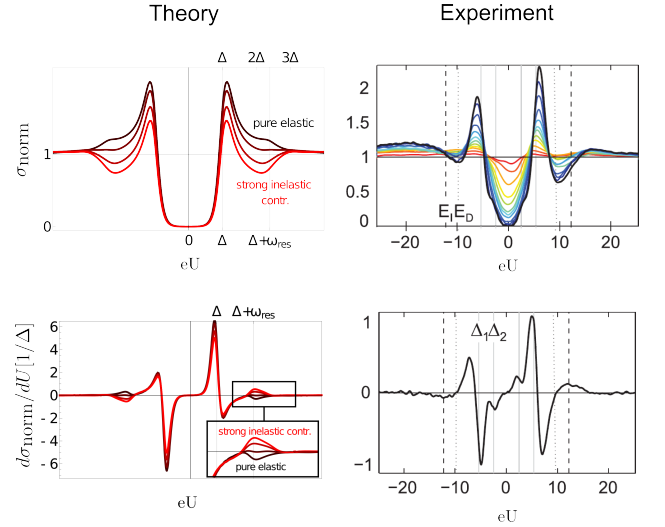
for energies $eU < \Delta + \omega_{res}$ (see Fig. 3 (a) and (b)). The obtained spectra look similar to many measured differential conductances [10, 13, 15–23], especially the fact that the superconducting differential conductance dips lie below the normal state differential conductance above the quasiparticle peak, followed by a V-shaped background conductance at higher energies.

As a specific example, we compare our theory with available experimental data we consider LiFeAs from Ref. [13, 14] (see right panel of Fig.4, where the black curve is at $2\,\mathrm{K}$ and should be compared to theoretical predictions in the left panel). In this case, just like in many high-temperature superconductors, the electronic spectrum in the normal state is non-flat. Thus, already in the normal state the elastic conductance shows a clear energy-dependence around the Fermi edge. One way to treat this is to normalize the experimental spectra with the normal state conductance. This normalization was used in Ref. [13]. In Fig. 4a we plot the normalized conductance $\sigma_{\mathrm{norm}}(U) = \sigma_{\mathrm{sc}}(U)/\sigma_{\mathrm{nc}}(\sqrt{U^2-(\Delta/e)^2})$, which facilitates a direct comparison with experiments as the effects of broken particle-hole symmetry is reduced noticeably. Even the detailed fine structures above the largest gap are fully consistent with the behaviour seen in our theory including inelastic tunneling (note that the experimental peak in the second derivative appears at energy

$\approx 2.4\Delta$ consistent with a neutron resonance mode below 2Δ [46, 48–50]). A significant loss of tunneling spectral weight can be seen in the superconductor for voltages $eU < \Delta + \omega_{res}$, especially at $eU \approx 2\Delta$, and a following strong increase of the normalized conductance due to inelastic contributions from the scattering off the resonance mode. In the normalized second derivative this gives rise to a peak at $eU \approx \Delta + \omega_{res}$ as also seen in the experimental data. Note, that for the pure elastic theory one expects a dip at this position. Thus, we conclude that inelastic tunneling is present here and that the pairing state of this system must be sign-changing, corresponding to an unconventional mechanism for superconductivity with a pairing interaction that dramatically reorganizes as one enters the superconducting state. In addition, the obtained normalized spectrum fits well with tunneling data for various other iron based superconductors [13, 24, 25] and cuprate superconductors [15, 20, 21, 54], except for the conductance in the gap region $eU < \Delta$ due to possible double gaps or nodes of the gap.

In summary, we demonstrated that a quantitative description of STM tunneling spectra of unconventional superconductors requires the inclusion of both, elastic and inelastic tunneling events. In the latter case a tip electron tunnels into an off-shell state and eventually relaxes to the Fermi energy by exciting a collective mode. This has long been demonstrated to be of importance in the normal state. Here we show that inelastic tunneling events are responsible for the frequently observed peak-dip features seen in STM spectra in the superconducting state of iron-based and cuprate materials. We utilize the fact that inelastic tunneling is directly related to momentum averaged bosonic excitations and demonstrate specifically that the much discussed system LiFeAs is governed by an electronic pairing mechanism with sign changing gap. To this end we performed explicit calculations of the elastic and inelastic tunneling spectrum for a spin-fluctuation induced pairing state that show striking similarities with the experimental data. Thus, inelastic tunneling offers a new spectroscopic approach to identify and constrain the collective modes that are responsible for unconventional superconductivity.

---

[1] W. McMillan and J. Rowell, Phys. Rev. Lett. 14, 108 (1965).

[2] W. L. McMillan, Phys. Rev. 167, 331 (1968).

[3] J. Hoffman, K. McElroy, D.-H. Lee, K. Lang, H. Eisaki, S. Uchida, and J. Davis, Science 297, 1148 (2002).

[4] P. Roushan, J. Seo, C. V. Parker, Y. Hor, D. Hsieh, D. Qian, A. Richardella, M. Z. Hasan, R. Cava, and A. Yazdani, Nature 460, 1106 (2009).

[5] A. Kreisel, P. Choubey, T. Berlijn, W. Ku, B.M. Andersen, and P.J. Hirschfeld, Phys. Rev. Lett. 114, 217002 (2015).

[6] J. Bardeen, Phys. Rev. Lett. 6, 57 (1961).

[7] M. H. Cohen, L. M. Falicov, and J. C. Phillips, Phys. Rev. Lett. 8, 316 (1962).

[8] G. Eliashberg, Sov. Phys JETP 12, 1000 (1961).

[9] J.F. Zasadzinski, L. Coffey, P. Romano, and Z. Yusof, Phys. Rev. B 68, 180504 (2003).

[10] F. Niestemski, S. Kunwar, S. Zhou, S. Li, H. Ding, Z. Wang, P. Dai, and V. Madhavan, Nature 450, 1058 (2007).

[11] L. Shan, J. Gong, Y.-L. Wang, B. Shen, X. Hou, C. Ren, C. Li, H. Yang, H.-H. Wen, S. Li, et al., Phys. Rev. Lett. 108, 227002 (2012).

[12] C.-L. Song, Y.-L. Wang, Y.-P. Jiang, Z. Li, L. Wang, K. He, X. Chen, J. E. Hoffman, X.-C. Ma, and Q.-K. Xue, Phys. Rev. Lett. 112, 057002 (2014).

[13] S. Chi, S. Grothe, R. Liang, P. Dosanjh, W.N. Hardy, S.A. Burke, D.A. Bonn, and Y. Pennec, Phys. Rev. Lett. 109, 087002 (2012).

[14] P. K. Nag, R. Schlegel, D. Baumann, H.-J. Grafe, R. Beck, S. Wurmehl, B. Bãijchner and C. Hess, Scientific Reports 6, 27926 (2016)

[15] J. M. Valles, R. C. Dynes, A. M. Cucolo, M. Gurvitch, L. F. Schneemeyer, J. P. Garno, and J. V. Waszczak, Phys. Rev. B 44, 11986 (1991).

[16] A. M. Cucolo, R. Di Leo, A. Nigro, P. Romano, and F. Bobba, Phys. Rev. B 54, R9686 (1996).

[17] S. Misra, S. Oh, D. J. Hornbaker, T. DiLuccio, J. N. Eckstein, and A. Yazdani, Phys. Rev. Lett. 89, 087002 (2002).

[18] M. Nishiyama, G. Kinoda, S. Shibata, T. Hasegawa, N. Koshizuka, and M. Murakami, Journal of Superconductivity 15, 351 (2002).

[19] I. Maggio-Aprile, C. Renner, A. Erb, E. Walker, and Ø. Fischer, Phys. Rev. Lett. 75, 2754 (1995).

[20] C. Renner, B. Revaz, K. Kadowaki, I. Maggio-Aprile, and Ø. Fischer, Phys. Rev. Lett. 80, 3606 (1998).

[21] P. Seidel, A. Plecenik, M. Grajcar, M. Belogolovskii, K.-U. Barholz, and A. Matthes, Physica C: Superconductivity 282, 1481 (1997).

[22] S. Matsuura, T. Taneda, W. Yamaguchi, H. Sugawara, T. Hasegawa, and K. Kitazawa, Physica C: Superconductivity 300, 26 (1998).

[23] J. Jandke, P. Wild, M. Schackert, S. Suga, T. Kobayashi, S. Miyasaka, S. Tajima, and W. Wulfhekel, Phys. Rev. B 93, 104528 (2016).

[24] Y. Fasano, I. Maggio-Aprile, N. Zhigadlo, S. Katrych, J. Karpinski, and Ø. Fischer, Phys. Rev. Lett. 105, 167005 (2010).

[25] Z. Wang, H. Yang, D. Fang, B. Shen, Q.-H. Wang, L. Shan, C. Zhang, P. Dai, and H.-H. Wen, Nature Phys. 9, 42 (2013).

[26] M. Eschrig and M. R. Norman, Phys. Rev. Lett. 85, 3261 (2000).

[27] A. Abanov and A. V. Chubukov, Phys. Rev. B 61, R9241 (2000).

[28] D. Manske, I. Eremin, and K. H. Bennemann, Phys. Rev. B 63, 054517 (2001).

[29] C. Berthod and T. Giamarchi, Phys. Rev. B 84, 155414 (2011).

[30] J. M. Rowell, W. L. McMillan, and W. L. Feldmann, Phys. Rev. 180, 658 (1969).

[31] M. Schackert, T. Märkl, J. Jandke, M. Hölzer, S. Ostanin, E.K.U. Gross, A. Ernst, and W. Wulfhekel, Phys. Rev. Lett. 114, 047002 (2015).

[32] See Supplemental Material: https://arxiv.org/pdf/1603.05288.pdf, which includes Refs. [33, 34].

[33] J. Jandke, P. Hlobil, M. Schackert, W. Wulfhekel, and J. Schmalian, Phys. Rev. B 93, 060505 (2016).

[34] Morel, P. & Anderson, P. W. Calculation of the Superconducting State Parameters with Retarded Electron-Phonon Interaction. *Phys. Rev.* **125**, 1263-1271 (1962).

[35] J. R. Kirtley and D. J. Scalapino, Phys. Rev. Lett. 65, 798 (1990).

[36] J. R. Kirtley, Phys. Rev. B 47, 11379 (1993).

[37] P. B. Littlewood and C. M. Varma, Phys. Rev. B 45, 12636 (1992).

[38] J. Lee, K. Fujita, K. McElroy, J. A. Slezak, M. Wang, Y. Aiura, H. Bando, M. Ishikado, T. Masui, J.-X. Zhu, A. V. Balatsky, H. Eisaki, S. Uchida, and J. C. Davis, Nature **442**, 546 (2006).

[39] M.-w. Xiao and Z.-z. Li, Physica C: Superconductivity 221, 136 (1994).

[40] K.-H. Bennemann and J. B. Ketterson, Superconductivity: Volume 1: Conventional and Unconventional Superconductors (Springer Science & Business Media, 2008).

[41] A. Abanov, A. V. Chubukov, and J. Schmalian, Journal of Electron Spectroscopy and Related Phenomena 117, 129 (2001).

[42] A. Abanov, A. V. Chubukov, and J. Schmalian, Europhys. Lett. 55, 369 (2001).

[43] R. M. Fernandes, private communication.

[44] A. Abanov and A. V. Chubukov, Phys. Rev. Lett. 83, 1652 (1999).

[45] P. Bourges, L. Regnault, J. Henry, C. Vettier, Y. Sidis, and P. Burlet, Physica B: Condensed Matter 215, 30 (1995).

[46] D. Inosov, J. Park, P. Bourges, D. Sun, Y. Sidis, A. Schneidewind, K. Hradil, D. Haug, C. Lin, B. Keimer, et al., Nature Phys. 6, 178 (2010).

[47] N.B. Christensen, D.F. McMorrow, H.M. Ronnow, B. Lake, S.M. Hayden, G. Aeppli, T.G. Perring, M. Mangkorntong, M. Nohara, and H. Takagi, Phys. Rev. Lett. 93, 147002 (2004).

[48] G. Yu, Y. Li, E. Motoyama, and M. Greven, Nature Phys. 5, 873 (2009).

[49] Rossat-Mignod and L. Regnault, Physica C: Superconductivity and Its Applications (Amsterdam, Netherlands) 185-189, 86 (1991).

[50] P. Bourges, H. F. Fong, L. P. Regnault, J. Bossy, C. Vettier, D. L. Milius, I. A. Aksay, and B. Keimer, Phys. Rev. B 56, R11439 (1997).

[51] T. Dahm, V. Hinkov, S. Borisenko, A. Kordyuk, V. Zabolotnyy, J. Fink, B. Buechner, D. Scalapino, W. Hanke, and B. Keimer, Nature Phys. 5, 217 (2009).

[52] J. Yang, J. Hwang, E. Schachinger, J.P. Carbotte, R.P.S.M. Lobo, D. Colson, A. Forget, and T. Timusk, Phys. Rev. Lett. 102, 027003 (2009).

[53] S. Dal Conte, C. Giannetti, G. Coslovich, F. Cilento, D. Bossini, T. Abebaw, F. Banfi, G. Ferrini, H. Eisaki, M. Greven, et al., Science 335, 1600 (2012).

[54] N. Jenkins, Y. Fasano, C. Berthod, I. Maggio-Aprile, A. Piriou, E. Giannini, B. W. Hoogenboom, C. Hess, T. Cren, and Ø. Fischer, Phys. Rev. Lett. 103, 227001 (2009).

[55] Note, that as usual STM probes the uppermost layers of a bulk system.